Communication

Double-Sided SIW Leaky-Wave Antenna With Increased Directivity in the E-Plane

Alejandro Javier Martinez-Ros, Maurizio Bozzi, and Marco Pasian

***Abstract*— The control of the radiation properties of a double-sided leaky-wave antenna (LWA) is demonstrated in this communication. To this aim, a standard substrate integrated waveguide (SIW) transmission line working with the TE_{20} mode is used. Due to the asymmetry of the radiated fields at both sides of the SIW, the equivalent magnetic currents generated are added in-phase at the center of the antenna, thus contributing to the radiation and improving the directivity in the E-plane. Moreover, the complex propagation constant of the SIW LWA is properly controlled by means of the separation P between posts, which mainly determines the leakage rate, and by the width W of SIW, which mainly determines the pointing angle. In order to demonstrate this control, three prototypes radiating at different pointing angles (10°, 30°, and 50°) and same beamwidth (10°) have been manufactured and measured at the design frequency of 15 GHz.**

***Index Terms*— Complex propagation constant, E-plane directivity, leaky-wave antenna (LWA), leaky-mode control, substrate integrated waveguide (SIW).**

I. Introduction

Leaky-Wave Antennas (LWAs) are a type of antennas whose radiation properties are mainly determined by the complex propagation constant of a leaky mode. Depending on the kind of structure used LWAs can show different radiation characteristics [1], which can be modified by controlling the leaky mode of the antenna. Due to the advantageous properties of high gain and easiness of integration with other structures, LWAs have received a large interest throughout the years and have been developed on almost any type of transmission line [1]. Particular interest has received the design of LWAs in planar form, due to a higher versatility for being used in different scenarios, such as automotive radars [2]–[4], indoor communications [5]–[7], or over conformal surfaces [8]–[10]. Typically, the radiation pattern of 1-D LWAs is equivalent to that of a single line-source, thus, only provides directivity along its longitudinal plane while showing a fan beam at the cross plane [1]. In order to increase the directivity at the cross plane, several antennas can be arranged forming an array [11]–[16]. Another alternative is to use a single LWA, but with two radiating line sources along the cross plane, which avoids the use of feeding networks. Some examples of this can be found in [17] and [18] for the first higher order mode of microstrip line, which only offers control over the phase constant (β) of the leaky mode, and in [19], for a substrate integrated waveguide (SIW) LWA, which uses the separation between posts of the SIW to radiate with the $n = -1$ Floquet space harmonic (SH), thus, not allowing the simultaneous control of the leakage rate (α) and the phase constant (β) of the leaky mode ($k = \beta - j\alpha$).

Manuscript received September 4, 2017; revised January 31, 2018; accepted February 21, 2018. Date of publication March 5, 2018; date of current version May 31, 2018. This work was supported in part by the Juan de la Cierva Program and in part by Ministerio de Ciencia e Innovación and European Union FEDER funds under Project TEC2013-41913-P. *(Corresponding author: Alejandro Javier Martinez-Ros.)*

A. J. Martinez-Ros is with the Dpto. de Física Aplicada 1, Universidad de Sevilla, 41012 Seville, Spain (e-mail: amartinez49@us.es).

M. Bozzi and M. Pasian are with the Department of Electrical, Computer and Biomedical Engineering, University of Pavia, 27100 Pavia, Italy (e-mail: maurizio.bozzi@unipv.it; marco.pasian@unipv.it).

Color versions of one or more of the figures in this communication are available online at http://ieeexplore.ieee.org.

Digital Object Identifier 10.1109/TAP.2018.2811843

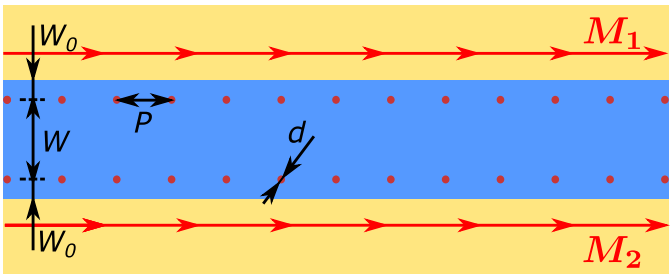

Fig. 1. Top view of the double-sided SIW LWA and its two equivalent magnetic currents M.

With the aim of overcoming this limitation, a recently proposed SIW LWA working with its TE_{20} mode [20] (see top view in Fig. 1) has been used to demonstrate this independent control on α and β while increasing the directivity in the E-plane. In this way, the dimensions (W, P) of the SIW are chosen to set the leaky mode in the fast-wave region ($\beta/k_0 < 1$), thus, the antenna can radiate without the necessity of exciting SHs, which allows that the separation between posts P can be used to control the leakage rate and the width W of the SIW to control the phase constant [21]. As a result, one can obtain a control over the phase constant β and the leakage rate α at both radiating edges. Moreover, due to the field configuration of the TE_{20} mode, the radiating edges have opposite polarizations, which allows that the E-fields can be added in-phase at the center of the array, in contrast to the TE_{10} mode which would provide the same polarization at both radiating edges and thus a null at the center of the antenna [22].

The rest of this communication is organized as follows. Section II describes the radiation mechanism of the antenna and the control over the complex propagation constant. Also, it is shown how depending on the distance between radiating edges, different beamwidths for the E-plane can be obtained. The design of three different prototypes of the proposed antenna is shown in Section III and their measured results are shown in Section IV. Finally, the main conclusion of this comunication is summarized in Section V.

II. Analysis of the Double-Sided SIW LWA

The LWA proposed in this communication consists of an SIW working on its TE_{20}-like mode, which is controlled to radiate according to a prescribed specification. To this aim, the separation between posts P and the separation between rows W of the SIW are used. In particular, the distance W mainly determines the phase constant β, of the leaky mode, whereas the separation P between posts is responsible for the control over the leakage rate α. However, since these values of α and β are coupled, a simultaneous control

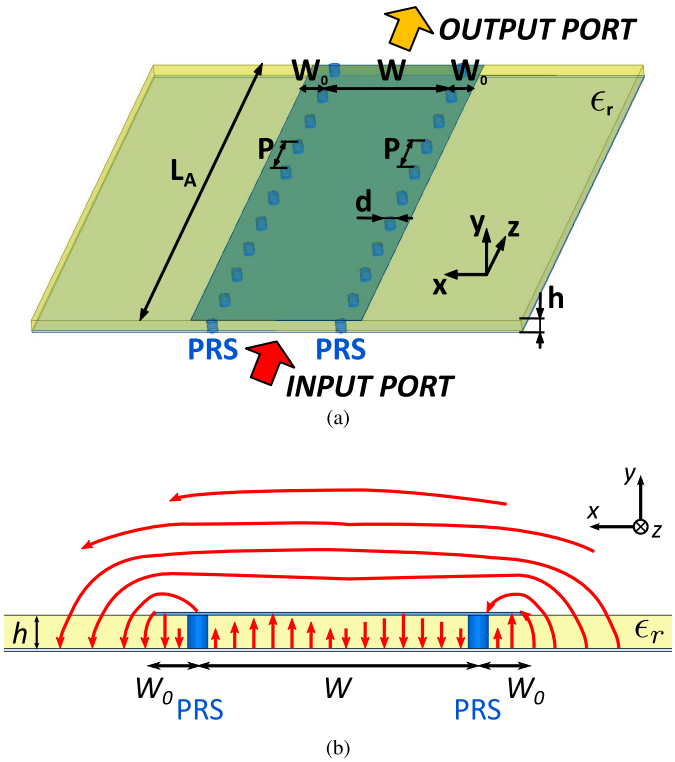

Fig. 2. Scheme of the double-sided SIW LWA. (a) 3-D view and main geometrical parameters. (b) Electric field distribution of the TE_{20} mode at the cross section of the antenna (E-plane).

over W and P is required to obtain the desired value of the complex propagation constant ($\gamma \equiv jk = \alpha + j\beta$). Due to the field distribution of the TE_{20} mode shown in Fig. 2(b), the antenna counts with the contribution of two radiating sides, which can be modeled as two magnetic currents M along the edges of the SIW LWA, as shown in Fig. 1. Moreover, since the width of the SIW LWA is $\approx \lambda_0$, the radiation of these magnetic currents M is added in-phase at the center of the antenna, as illustrated in Fig. 2(b).

It is important to note that although the proposed SIW LWA has the fundamental mode as TE_{10}, the TE_{20} is the only working one due to the suppression of the TE_{10} mode of the structure. As a result, the antenna can be considered as single mode, which allows for a simpler analysis of the structure.

In this way, the complex propagation constant of this TE_{20} mode can be expressed as

$$k_z(z) = \beta_z(z) - j\alpha_z(z) \tag{1}$$

where β_z stands for the phase constant and α_z for the leakage rate along the z-axis. Moreover, the radiated pointing angle $\theta_{\text{RAD}}(z)$ can be determined by relating β_z with the free-space wavenumber $k_0 = 2\pi/\lambda_0$ [1]

$$\sin\theta_{\text{RAD}}(z) \approx \beta_z(z)/k_0. \tag{2}$$

On the other hand, the beamwidth $\Delta\theta$ can also be expressed as function of the antenna length L_A and θ_{RAD}

$$\Delta\theta \approx \frac{1}{\frac{L_A}{\lambda_0}\cos\theta_{\text{RAD}}}. \tag{3}$$

With θ_{RAD} and $\Delta\theta$ fixed, the antenna length L_A can be obtained by using (3). Then, the leakage rate α is determined for a 90% radiation efficiency ($\eta_{\text{RAD}} = 1 - e^{-2\alpha L_A}$) [1], staying the leaky mode completely determined for the required values of θ_{RAD} and $\Delta\theta$. For the proposed antenna, the desired values of α and β are obtained by varying the geometrical parameters (W and P) as described in [20] and [22]. As a consequence of this control, the radiation diagram of the leaky mode along its longitudinal plane can be determined by using (2) and (3). However, (2) and (3) are valid for obtaining the radiation pattern of a line-source LWA along its longitudinal plane, but not for the transverse plane, which typically has a fan beam. Moreover, the two radiating sides of the proposed antenna can be considered as two magnetic currents M along the length of the LWA and separated at a distance $x_d = W + 2W_0$ (see Fig. 1), which take the following form:

$$M(x,\ y,\ z) = \int_{-\infty}^{+\infty} A(x,\ y,\ z)\delta(x - |x_d|)e^{-jkz}dx \tag{4}$$

with $\delta(x - |x_d|)$ the Dirac delta function along x. Due to these two magnetic currents, the directivity at the transverse plane can be increased in more than 4 dB compared to single line-source antennas [22], thus providing a radiation pattern similar to the microstrip radiating with the first higher order mode [23] or the periodic LWA [19], but adding a control over both β and α. Since the leaky mode must fall into the fast-wave region ($\beta/k_0 < 1$) to radiate, the separation between the two magnetic currents for the TE_{20} mode is $\approx \lambda(= \lambda_0/\sqrt{\epsilon_r})$, thus $< \lambda_0$, which only allows a single main beam in the radiation pattern [24]. Moreover, since this separation between magnetic currents mainly depends on the substrate permittivity, some different beamwidths in the E-plane can be obtained by increasing or decreasing this distance.

The radiation pattern of a single line-source can be seen as the sum of infinite point sources, which provides directivity along its longitudinal plane but a fan beam at the transverse plane. However, for the case of two line-sources ($M = 2$) separated at a distance x_d this directivity for the transverse plane can be increased by the addition of two radiating sources. Moreover, if the spacing between elements is small enough ($\approx \Delta z < \lambda_0/10$) the continuous line-source can be discretized and represented as a sum of multiple point sources separated at a distance Δz. As a result, the radiation pattern of this configuration can be well approximated by using array theory [24], and its array factor can be expressed as

$$AF(\theta,\ \phi) = \sum_{m=1}^{M} I_{xm}e^{\xi_{xm}} \cdot \sum_{n=1}^{N} I_{zn}e^{\xi_{zn}} \tag{5}$$

where

$$\xi_{xm} = jkx_m \sin\theta\cos\phi + \Phi_x \tag{6}$$

$$\xi_{zn} = jkz_n \sin\theta\sin\phi + \Phi_z \tag{7}$$

and Φ_z and Φ_x stand for the phase shift between elements, and M and N for the number of elements considered along each direction (in our case $M = 2$ and $N = 10\ L_A/\lambda_0$).

III. Design of the Double-Sided SIW LWA

The proposed control over the propagation constant is demonstrated with the design of several prototypes, which have different pointing angles ($\theta_{\text{RAD}} = 10°$, 30°, and 50°) and the same beamwidth ($\Delta\theta = 10°$). A schematic view of the complete structure, including the feeding and its main sections, is shown in Fig. 3. In particular, the following three main parts can be distinguished as:

1) port 1, input port from a coaxial probe and excitation of the TE_{20} mode of the SIW, L_0;
2) radiating length of the LWA, L_A;
3) port 2, output port from the SIW with TE_{20} mode to the coaxial probe, L_0.

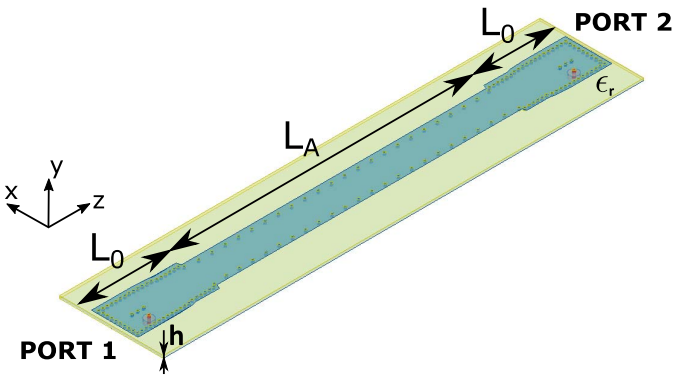

Fig. 3. Scheme of the SIW LWA including feeding ports and main sections.

TABLE I

PHYSICAL DIMENSIONS FOR THREE PLANAR LWA WITH DIFFERENT POINTING ANGLES AND A CONSTANT BEAMWIDTH ($\eta_{\text{RAD}} = 90\%$)

θ_{RAD}	$\Delta\theta$	$L_A(mm)$	$W(mm)$	$P(mm)$
10°	10°	117	12.85	4.5
30°	10°	129.49	12.31	5.63
50°	10°	175.5	11.85	6.75

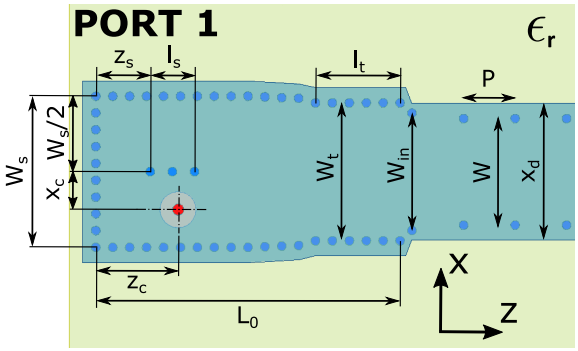

Fig. 4. Detailed view of the feeding together with its main geometrical dimensions.

All structures have been designed to radiate 90% of the energy at the end of the antenna and the main geometrical dimensions for the three proposed antennas are summarized in Table I. Due to the proposed antenna works with the TE_{20} mode, first, it is necessary to design a feeding that allows the excitation of the TE_{20} mode and the suppression of the TE_{10}. To this aim, the antenna is fed with a coaxial probe whose inner conductor passes through the substrate and then is soldered at the top layer. A detailed view of the transition and its main geometrical dimensions is shown in Fig. 4. It can be seen that the coaxial probe is shifted $x_c = W_s/4 = 4.25$ mm from the center, as a result of the field distribution of the TE_{20} mode that has its maximum intensity at $\pm W_s/4$ from the center [25]. Also, it is observed that the width of the SIW transition (with length L_0) is tapered in order to match the phase constant of the SIW LWA, in this manner, the width is varied from $W_s = 17$ mm to different values of W_t for each prototype while the separation between posts is kept constant at 1.9 mm. In addition to the coaxial probe, a central row with three metallic posts of diameter $d = 1$ mm and length $l_s = 5$ mm is placed at center of the SIW to suppress the TE_{10} mode. The designed feeding, whose geometrical parameters schemed in Fig. 4 summarize in Table II, provides an isolation for the TE_{10} mode larger than 15 dB at the design frequency of 15 GHz (for all designs), thus, resulting very useful for this purpose because of the compactness and the absence of radiation losses inherent to feeding types based on microstrip lines [26]. However, it is also worth noting that this type of feeding based on coaxial probes are usually narrowband, because of the mismatch between the coaxial and the SIW.

TABLE II

MAIN PHYSICAL DIMENSIONS (IN MILLIMETER) OF THE FEEDING FOR THE TE_{20} MODE FOR THREE SIW LWA WITH CONSTANT $\Delta\theta = 10°$

θ_{RAD}	z_c	z_s	W_t	W_{in}	l_t	x_s	L_0
10°	8.8	6.1	16	16	12.85	4.75	34.2
30°	9.25	6.1	15.8	16	12.31	5.63	34.2
50°	9.25	6.1	15.3	16	11.85	6.75	34.2

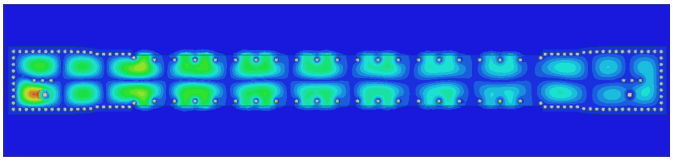

Fig. 5. Simulated E-field along the SIW LWA at the design frequency of 15 GHz.

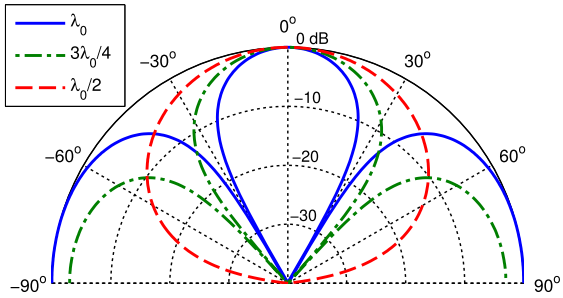

Fig. 6. Array factor of two infinitesimal dipoles separated at λ_0, $3\lambda_0/4$, and $\lambda_0/2$.

Fig. 5 shows the simulated E-field distribution obtained for one of the antennas at the design frequency of 15 GHz. In particular, it can see that the TE_{20} is the dominant mode in the structure, and that is correctly excited with the feeding shown in Fig. 4. It is also observed the leakage of energy, represented by the lower intensity of the fields along the propagation direction of the antenna.

Another characteristic that needs to be taken into account for this type of antennas is the distance between the two radiating edges. As stated in (5), the two radiating edges can be seen as two line-sources separated at a distance $x_d = W + 2W_0$. Therefore, depending on this distance different radiation patterns in the E-plane can be obtained. However, this distance cannot be arbitrarily set since varying it, also changes the β of the leaky mode and its pointing angle. Moreover, the distance W_0 needs to be lower than $\approx \lambda/4$ in order to avoid the propagation of channel modes [27]. Nevertheless, an alternative to control this distance x_d between radiating edges is to use different substrate permittivities for the antenna, due to the separation between edges is $\approx \lambda_0/\sqrt{\epsilon_r}$ for the TE_{20} mode, but at the expense of increasing the phase-constant dispersion [28].

In order to clarify this point, Fig. 6 shows the ideal radiation pattern of two infinitesimal dipoles separated at different distances [24]. These ideal radiation patterns provide a good approximation of the E-plane ($\theta = 0°$) radiation pattern of the proposed antenna, since

TABLE III

MAIN PARAMETERS AT THE DESIGN FREQUENCY OF 15 GHz FOR AN ARRAY OF TWO ELEMENTS WITH DIFFERENT SUBSTRATE PERMITTIVITIES

x_d	distance(mm)	$\Delta\theta$	$\lambda(\epsilon_r)$ in mm
λ_0	20	29°	$\lambda(2.2) = 13.5$
$3\lambda_0/4$	15	39°	$\lambda(4.5) = 9.4$
$\lambda_0/2$	10	60°	$\lambda(6) = 8.2$

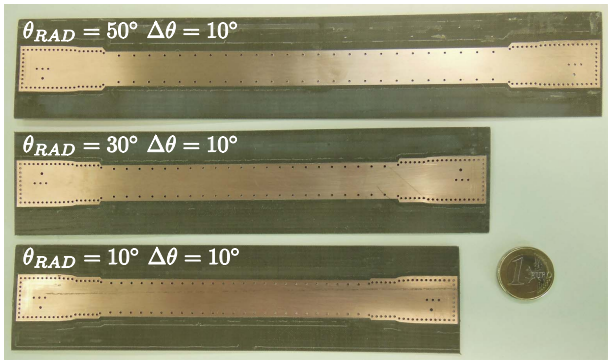

Fig. 7. Photograph of the three manufactured prototypes radiating at different pointing angles at the design frequency of 15 GHz.

the radiating edges can be seen as infinitesimal sources separated at a distance $x_d = W + 2W_0$. Nevertheless, due to the 2-D distribution of the array, this E-plane shown in Fig. 6 must be multiplied by the array factor along the longitudinal direction [see (5)] in order also to take into account the contributions along this direction. As shown in Fig. 6, the beamwidth $\Delta\theta$ is reduced as the distance between elements is increased, however, the sidelobe level also increases. The main parameters regarding to this two elements array are summarized in Table III. In particular, the beamwidth $\Delta\theta$ for different separation between elements (x_d) is shown. Moreover, due to the proposed SIW LWA has a separation between edges of $\approx \lambda(= \lambda_0/\sqrt{\epsilon_r})$, the corresponding values of λ for different ϵ_r are also shown (column IV). In this manner, it can be seen that for a substrate permittivity with $\epsilon_r = 2.2$ ($\lambda = 13.5$ mm) the beamwidth for the E-plane ($\theta = 0°$) corresponds to $\Delta\theta \approx 39°$ ($x_d = 15$ mm).

IV. RADIATION PATTERNS

The designs proposed in Section III have been manufactured and measured for a design frequency of 15 GHz. A commercial substrate RT/duroid 5880 ($h = 0.508$ mm, $\epsilon_r = 2.2$, and $\tan\delta = 0.0009$) has been used. Here, the measured results are compared to the simulated ones in order to demonstrate the theoretical concepts presented along this communication. In particular, the radiation patterns for the three antennas proposed are shown at both E- and H-planes. Moreover, the gain values and the input matching are also shown.

A photograph of the three manufactured prototypes is shown in Fig. 7. It can be observed that the three designs have different lengths, due to the fact that the antennas have been designed with the same radiation efficiency ($\eta_{\text{RAD}} \approx 90\%$) and with different pointing angles but the same beamwidth (3). In Fig. 8, it is shown that for the design frequency of 15 GHz, the radiation patterns at the H-plane (yz-plane) for these three antennas. Measured results (solid lines) are compared to the simulated ones (dashed lines) and very good agreement is obtained for all cases, demonstrating the control over α and β for the proposed SIW LWA working with the TE_{20} mode. Moreover, the radiation patterns for the E-plane are also represented in Fig. 9. Due to the E-plane is defined along the angle of maximum

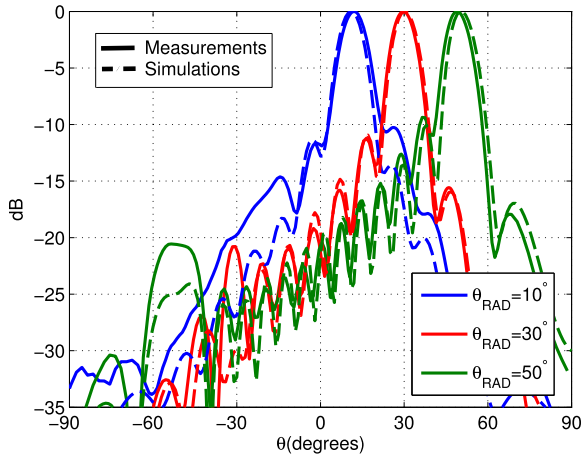

Fig. 8. Measured and simulated normalized H-plane ($\phi = 90°$) radiation patterns at 15 GHz for the thee antennas summarized in Table I.

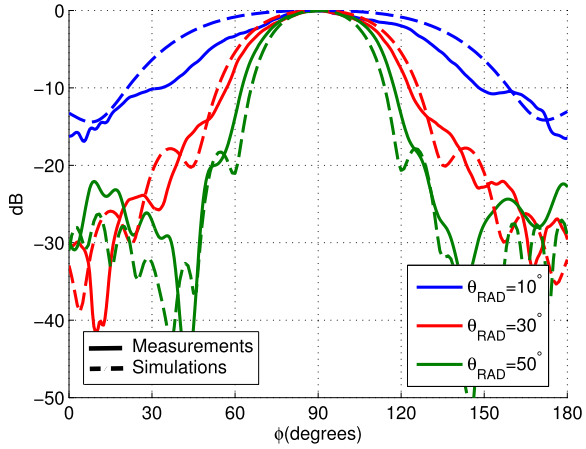

Fig. 9. Measured and simulated normalized E-plane radiation patterns at 15 GHz for the thee antennas summarized in Table I.

TABLE IV

GAIN AND BEAMWIDTH IN THE E-PLANE FOR THE THREE PROPOSED ANTENNAS AT THE DESIGN FREQUENCY OF 15 GHz

θ_{RAD}	$\Delta\theta$	$x_d(mm)$	Gain(dB)
10°	63°	16.25	14.1
30°	43°	15.71	15.1
50°	38°	15.25	14.9

radiation (θ_{RAD}) of each SIW LWA, the three antennas have been measured according to them for the values of ϕ from 0° to 180°. Measured results (solid lines) are compared to the simulated ones (dashed lines) for all the cases and good agreement is obtained. In particular, it can be seen in blue, the E-plane for the SIW LWA radiating at $\theta_{\text{RAD}} = 10°$, in red, the one radiating at $\theta_{\text{RAD}} = 30°$, and in green, the one at $\theta_{\text{RAD}} = 50°$. In Table IV, the main values of each antenna for this E-plane are summarized. Specifically, the beamwidth $\Delta\theta$ at -3 dB, the separation between radiating sides x_d and the gain.

Finally, with the aim of providing a better knowledge about some radiation properties of the proposed antennas, a more detailed view for one of the prototypes (antenna pointing at $\theta_{\text{RAD}} = 30°$) is given. In particular, the radiation patterns for both E- and H-plane, and the $|S|$-parameters are represented in Figs. 10–12.

In Fig. 10, it can be seen the radiation pattern for the H-plane at the design frequency of 15 GHz. In particular, it is observed that the measured (in solid lines) and simulated (in dashed lines) co-pol (blue

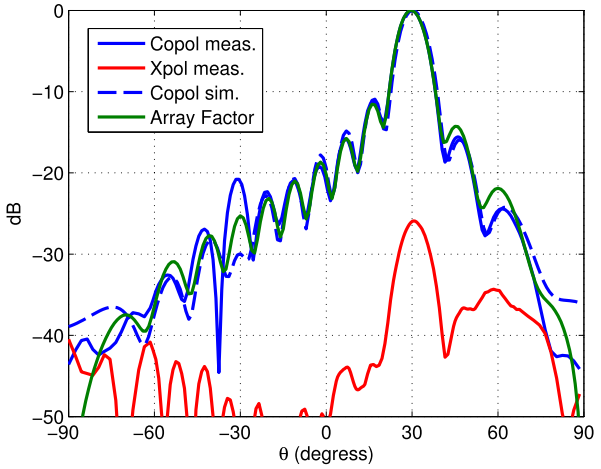

Fig. 10. Co-pol and x-pol components for the normalized H-plane ($\phi = 90°$) radiation pattern at 15 GHz for the SIW LWA pointing at $\theta_{\mathrm{RAD}} = 30°$.

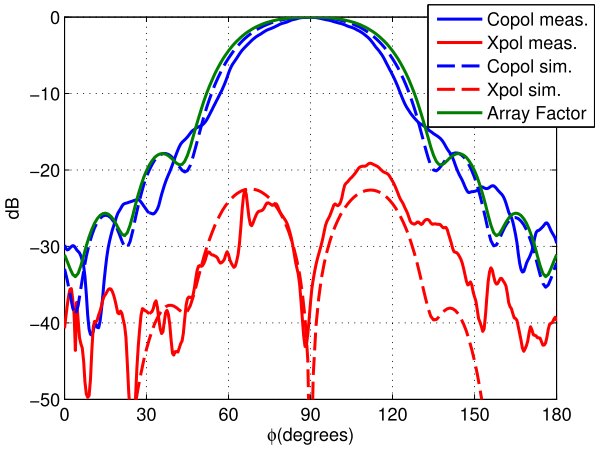

Fig. 11. Co-pol and x-pol components for the normalized E-plane ($\theta = 30°$) radiation pattern at 15 GHz for the SIW LWA pointing at $\theta_{\mathrm{RAD}} = 30°$.

line) and x-pol (red line) components for the SIW LWA pointing at $\theta_{\mathrm{RAD}} = 30°$. Moreover, the radiation pattern from the array factor described in (5), which is multiplied by a cosine factor to consider the ground plane effect [24], is also shown in green line. It can be seen a very good agreement for all curves, with the exception of the simulated x-pol component that is below -60 dB (not shown in Fig. 10), demonstrating the suitable control over the leaky mode in this SIW LWA operating with the TE_{20}.

The E-plane radiation pattern measured at $\theta = 30°$ is also shown in Fig. 11. Again, it can be seen a very good agreement for all components including the measured and simulated x-pol components (red lines), which are below -20 dB for the whole range of ϕ. In addition, the array factor (green line) obtained with (5) provides a very good agreement for the co-pol component. Moreover, it is observed that the co-pol component (solid blue line) has a -3 dB beamwidth of $\Delta\theta = 43°$ and a maximum gain of 15.1 dB, as summarized in Table IV.

In Fig. 12, the |S|-parameters for a frequency range from 13.5 to 16.5 GHz are shown. Measured results are in solid lines and the simulated ones are in dashed lines. It is observed that the $|S_{11}|$ (blue line) is below -17 dB for the design frequency of 15 GHz, whereas the $|S_{21}|$ (red line) is -11 dB confirming the high radiation efficiency of the proposed antenna. Moreover, it can be seen that the

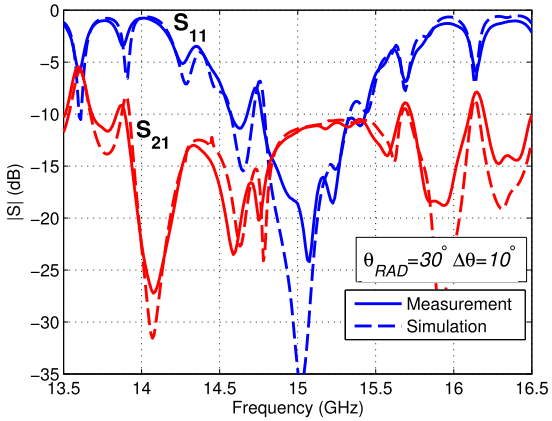

Fig. 12. Measured and simulated |S|-parameters for the SIW LWA pointing at $\theta_{\mathrm{RAD}} = 30°$ at the design frequency of 15 GHz.

proposed antenna has a narrowband ($\approx 3\%$) below -10 dB because of the compact feeding used for exciting the TE_{20} mode. For wider bandwiths more standard configurations based on branch lines [25] could be used at the expense of increasing the size of the device.

V. Conclusion

An innovative design of SIW LWA with capability to radiate from both sides of the SIW line has been presented. In this manner, a higher directivity at the transverse plane compared to single line-source antennas is achieved. The SIW LWA uses the TE_{20} mode of the SIW as the working one. To this aim, the TE_{10} mode is suppressed by using a compact feeding from a coaxial through line. By means of the geometrical parameters (W, P) of the SIW, the leaky mode ($k = \beta - \mathrm{j}\alpha$) of the SIW LWA is suitably controlled. This control has been experimentally demonstrated by means of three antennas radiating at three different pointing angles ($\theta_{\mathrm{RAD}} = 10°$, $30°$, and $50°$) and the same beamwidth ($\Delta\theta = 10°$) for the design frequency of 15 GHz. Measured results have been compared with results obtained with commercial full-wave software and with theoretical ones and good agreement is found for both E- and H-planes validating the theoretical concepts exposed along the communication.

Acknowledgment

The authors would like to thank Prof. A. Mennella, Dr. C. Franceschet, and J. Martelli from the Department of Physics, University of Milan, Milan, Italy, for their precious support during the antenna measurements in the anechoic chamber.

References

[1] A. A. Oliner and D. R. Jackson, "Leaky-wave antennas," in *Antenna Engineering Handbook*, 4th ed. J. L. Volakis, Ed. New York, NY, USA: McGraw-Hill, Jun. 2007, ch. 11.

[2] K. Sato, S.-I. Matsuzawa, and Y. Inoue, "Composite right/left-handed leaky wave antenna for millimeter-wave automotive applications," in *Proc. 1st Eur. Conf. Antennas Propag.*, Nov. 2006, pp. 1–4.

[3] M. Ettorre, R. Sauleau, L. L. Coq, and F. Bodereau, "Single-folded leaky-wave antennas for automotive radars at 77 GHz," *IEEE Antennas Wireless Propag. Lett.*, vol. 9, pp. 859–862, 2010.

[4] W. Cao, Z. N. Chen, W. Hong, B. Zhang, and A. Liu, "A beam scanning leaky-wave slot antenna with enhanced scanning angle range and flat gain characteristic using composite phase-shifting transmission line," *IEEE Trans. Antennas Propag.*, vol. 62, no. 11, pp. 5871–5875, Nov. 2014.

[5] I. Ohtera, "On a forming of cosecant square beam using a curved leakywave structure," *IEEE Trans. Antennas Propag.*, vol. 49, no. 6, pp. 1004–1006, Jun. 2001.

[6] Y. P. Zhang, "Indoor radiated-mode leaky feeder propagation at 2.0 GHz," *IEEE Trans. Veh. Technol.*, vol. 50, no. 2, pp. 536–545, Mar. 2001.
[7] M. Nakamura, H. Takagi, K. Einaga, T. Nishikawa, N. Moriyama, and K. Wasaki, "Development of a 300 m 2.4 GHz frequency band leaky coaxial cable for wireless network access," in *Proc. IEEE Radio Wireless Symp.*, Jan. 2008, pp. 687–690.
[8] O. Losito, "Design of conformal tapered leaky wave antenna," in *Proc. Progr. Electromagn. Res. Symp.*, Prague, Czech Republic, Aug. 2007, pp. 177–181.
[9] M. Hashemi and T. Itoh, "Dispersion engineered metamaterial-based transmission line for conformal surface application," in *IEEE MTT-S Int. Microw. Symp. Dig.*, Atlanta, Ga, USA, Jun. 2008, pp. 331–334.
[10] A. J. Martinez-Ros, J. L. Gomez-tornero, and G. Goussetis, "Conformal tapered substrate integrated waveguide leaky-wave antenna," *IEEE Trans. Antennas Propag.*, vol. 62, no. 12, pp. 5983–5991, Dec. 2014.
[11] J. Hirokawa and M. Ando, "Single-layer feed waveguide consisting of posts for plane TEM wave excitation in parallel plates," *IEEE Trans. Antennas Propag.*, vol. 46, no. 5, pp. 625–630, May 1998.
[12] T. Zhao, D. R. Jackson, J. T. Williams, H.-Y. D. Yang, and A. A. Oliner, "2-D periodic leaky-wave antennas—Part I: Metal patch design," *IEEE Trans. Antennas Propag.*, vol. 53, no. 11, pp. 3505–3514, Nov. 2005.
[13] M. Ettorre, A. Neto, G. Gerini, and S. Maci, "Leaky-wave slot array antenna fed by a dual reflector system," *IEEE Trans. Antennas Propag.*, vol. 56, no. 10, pp. 3143–3149, Oct. 2008.
[14] H. V. Nguyen, S. Abielmona, and C. Caloz, "Highly efficient leaky-wave antenna array using a power-recycling series feeding network," *IEEE Antennas Wireless Propag. Lett.*, vol. 8, pp. 441–444, 2009.
[15] S. K. Podilchak, L. Matekovits, A. P. Freundorfer, Y. M. M. Antar, and M. Orefice, "Controlled leaky-wave radiation from a planar configuration of width-modulated microstrip lines," *IEEE Trans. Antennas Propag.*, vol. 61, no. 10, pp. 4957–4972, Oct. 2013.
[16] A. J. Martinez-Ros, J. L. Goómez-Tornero, and G. Goussetis, "Pencil beam radiation pattern from a single-layer substrate-integrated waveguide leaky-wave antenna with simple feeding," *IET Microw. Georgia, Antennas Propag.*, vol. 9, no. 1, pp. 24–30, 2015.
[17] W. Menzel, "A new travelling wave antenna in microstrip," *Arch. Elektron. Uebertrag. Tech.*, vol. 33, no. 4, pp. 137–140, Apr. 1979.
[18] A. A. Oliner, "Leakage from higher modes on microstrip line with application to antennas," *Radio Sci.*, vol. 22, pp. 907–912, Nov. 1987.
[19] F. Xu, K. Wu, and X. Zhang, "Periodic leaky-wave antenna for millimeter wave applications based on substrate integrated waveguide," *IEEE Trans. Antennas Propag.*, vol. 58, no. 2, pp. 340–347, Feb. 2010.
[20] A. J. Martinez-Ros, M. Bozzi, M. Pasian, and F. Mesa, "Leaky-wave antenna in planar technology with high directivity in the transverse plane," in *Proc. 11th Eur. Conf. Antennas Propag. (EUCAP)*, Mar. 2017, pp. 3869–3871.
[21] M. Pasian, M. Bozzi, and L. Perregrini, "A formula for radiation loss in substrate integrated waveguide," *IEEE Trans. Microw. Theory Techn.*, vol. 62, no. 10, pp. 2205–2213, Oct. 2014.
[22] A. J. Martinez-Ros, J. L. Gomez-Tornero, and G. Goussetis, "Planar leaky-wave antenna with flexible control of the complex propagation constant," *IEEE Trans. Antennas Propag.*, vol. 60, no. 3, pp. 1625–1630, Mar. 2012.
[23] A. Oliner and K. Lee, "Microstrip leaky wave strip antennas," in *Proc. Antennas Propag. Soc. Int. Symp.*, vol. 24. Philadelphia, PA, USA, Jun. 1986, pp. 443–446.
[24] W. L. Stutzman and G. A. Thiele, *Antenna Theory and Design*. Hoboken, NJ, USA: Wiley, 2012.
[25] D. M. Pozar, *Microwave Engineering*, 2nd ed. Hoboken, NJ, USA: Wiley, 1998.
[26] M. Bozzi, A. Georgiadis, and K. Wu, "Review of substrate-integrated waveguide circuits and antennas," *IET Microw. Antennas Propag.*, vol. 5, no. 8, pp. 909–920, Jun. 2011.
[27] H. Shigesawa, M. Tsuji, P. Lampariello, F. Frezza, and A. A. Oliner, "Coupling between different leaky-mode types in stub-loaded leaky waveguides," *IEEE Trans. Microw. Theory Techn.*, vol. 42, no. 8, pp. 1548–1560, Aug. 1994.
[28] A. J. Martinez-Ros, J. L. Gomez-Tornero, and G. Goussetis, "Frequency scanning leaky wave antenna for positioning and identification of RFID tags," in *Proc. IEEE Int. Conf. RFID-Technol. Appl. (RFID-TA)*, Sitges, Spain, Sep. 2011, pp. 451–456.